9-28-2016

Polycyclic Musks in the Air and Water of the Lower Great Lakes: Spatial Distribution and Volatilization from Surface Waters

Carrie A. McDonough

Paul A. Helm

Derek Muir

Gavino Puggioni

Rainer Lohmann
University of Rhode Island, rlohmann@uri.edu

Citation/Publisher Attribution

Mcdonough, C. A., Helm, P. A., Muir, D., Puggioni, G., & Lohmann, R. (2016). Polycyclic Musks in the Air and Water of the Lower Great Lakes: Spatial Distribution and Volatilization from Surface Waters. *Environmental Science & Technology*, 50(21), 11575-11583.
Available at: http://pubs.acs.org/doi/abs/10.1021/acs.est.6b03657

Polycyclic Musks in the Air and Water of the Lower Great Lakes: Spatial Distribution and Volatilization from Surface Waters

Polycyclic Musks in the Air and Water of the Lower Great Lakes: Spatial Distribution and Volatilization from Surface Waters

Carrie A. McDonough[1], Paul A. Helm[2], Derek Muir[3], Gavino Puggioni[4], Rainer Lohmann[1*]

[1] University of Rhode Island, Graduate School of Oceanography, 215 S. Ferry Road, Narragansett, RI 02882, USA

[2] Ontario Ministry of the Environment and Climate Change, 125 Resources Road, Toronto, Ontario, Canada M9P 3V6

[3] Environment Canada, Aquatic Contaminants Research Division, 867 Lakeshore Road, Burlington, Ontario, Canada L7S 1A1

[4] University of Rhode Island, 45 Upper College Road, Kingston, RI 02881, USA

[*] Corresponding Author; Email: rlohmann@ uri.edu; Phone: 401-874-6612; Fax: 401-874-6811

ABSTRACT

Polycyclic musks (PCMs) are synthetic fragrance compounds used in personal care products and household cleaners. Previous studies have indicated that PCMs are introduced to aquatic environments via wastewater and river discharge. Polyethylene passive samplers (PEs) were deployed in air and water during winter 2011 and summer 2012 to investigate the role of population centers as sources of these contaminants to the Great Lakes and determine whether the lakes were acting as sources of PCMs via volatilization. Average gaseous Σ_5PCM ranged from below detection limits (<DL) to 3.2 ng/m^3 on the western shoreline of Lake Erie in Toledo. Average dissolved Σ_5PCM ranged from <DL to 2.6 ng/L on the southern shore of Lake Ontario near the mouth of the Oswego River. Significant correlations were observed between population density and Σ_5PCM in both air and water, with strongest correlations within a 25 and 40 km radius, respectively. At sites where HHCB was detected it was generally volatilizing, while the direction of AHTN air-water exchange was variable. Volatilization fluxes of HHCB ranged from 11±6 ng/m^2/day to 341±127 ng/m^2/day, while air-water exchange fluxes of AHTN ranged from -3±2 ng/m^2/day to 28±10 ng/m^2/day. Extrapolation of average air-water exchange flux values over the surface area of the lakes' coastal boundary zone suggested volatilization may be responsible for the loss of 64-213 kg/year of dissolved Σ_5PCM from the lakes.

INTRODUCTION

Polycyclic musks (PCMs) are ubiquitous pollutants widely used as additives in personal care products and household cleaners to lend them a long-lasting, pleasing odor.[1–3] Previous studies have indicated that PCMs are introduced to aquatic environments, including the Great Lakes, via effluent from wastewater treatment plants (WWTPs) and river discharge.[3–6] One of the most widely used PCMs, 1,3,4,6,7,8-hexahydro-4,6,6,7,8,8-hexamethylcyclopenta-(g)-2-benzopyran (HHCB, or Galaxolide®), was listed as one of Howard and Muir's top 50 high priority pollutants with persistence and bioaccumulation potential in need of increased monitoring.[7] The effects of PCMs on aquatic organisms are largely unknown, but they have been found to bioaccumulate[8–10] and recent studies suggest environmentally relevant concentrations may cause oxidative stress and genetic damage in some organisms.[11]

Polyethylene passive samplers (PEs) are promising tools for measuring hydrophobic organic contaminants (HOCs) at high spatial resolution because they are cost-effective, require no electricity, and are simple to deploy.[12] PEs sequester the dissolved or gaseous fraction of HOCs from the surrounding water or air over time, allowing measurement of time-integrated concentrations.[13–16] They have been used to measure a wide variety of HOCs in air and water and to calculate air-water exchange fluxes,[17–20] but they have not been applied to the study of air-water exchange for PCMs.

The use of PEs in this study provided a unique opportunity to measure the truly gaseous and dissolved fraction of PCMs available for air-water exchange and determine whether gaseous PCMs were volatilizing from surface waters in Lake Erie and Lake Ontario. Based on previous work, volatilization may be an important loss route for PCMs in the Great Lakes,[4,5] but fluxes

had not been determined by simultaneous air and water sampling. In this study, PEs were deployed in air and water during winter 2011 and summer 2012 to (i) measure baseline gaseous and dissolved concentrations of PCMs in and above Lakes Erie and Ontario, (ii) investigate the role of population centers as sources of these contaminants, (iii) determine whether the lakes were acting as sources of PCMs via volatilization, and (iv) explore how PE-derived PCM air-water exchange fluxes respond to non steady-state conditions.

METHODS

Sampler Preparation and Deployment. Prior to deployment, PEs were pre-extracted in solvent and loaded with performance reference compounds (PRCs) dibromobiphenyl, tetrabromobiphenyl, pentabromobiphenyl, naphthalene-*d8*, pyrene-*d10*, and benzo(a)pyrene-*d12* as described previously.[19] The PE deployment schedule and meteorological parameters, including the number of days each PE was deployed, are summarized in Supporting Information (SI) Table S1. Average temperature and wind speed were determined using data from the nearest available meteorological buoy (Table S2, Figure S1).

Shoreline PEs were deployed by trained volunteers as previously described.[19] Briefly, volunteers hung air PEs inside protective metal bowls at a height of about 1.5 meters, and tethered water PEs to an anchored line so that they would be secured about 1 meter beneath the water's surface. Offshore and nearshore deployments were carried out by workers at Environment Canada and the Ontario Ministry of the Environment, as described previously by Liu et al.[17] Air PEs were secured in a protective chamber 2 meters above the water's surface on a buoy and water PEs were enclosed within a perforated metal cage and secured to the buoy

about 4 meters below the water's surface. After the PEs were recovered, they were shipped back to the laboratory overnight on ice and frozen until extraction.

Extraction and Analysis. PEs from 56 atmospheric deployments (including 9 over-winter deployments) and 39 aqueous deployments were extracted and analyzed. All PEs were spiked with labeled PAHs (acenaphthene-*d10*, phenanthrene-*d10*, chrysene-*d12*, and perylene-*d12*) and extracted for 18-24 hours in pentane, concentrated to <100 μL, and spiked with injection standard p-terphenyl-*d14*. All extracts from aqueous PEs were passed through silica gel/sodium sulfate cleanup columns.

Extracts were analyzed for five PCMs: 1,3,4,6,7,8-hexahydro-4,6,6,7,8,8-hexamethylcyclopenta-(g)-2-benzopyran (HHCB, or Galaxolide®), 7-acetyl-1,1,3,4,4,6-hexamethyl-1,2,3,4-tetrahydronaphthalene (AHTN, or Tonalide®), 4-acetyl-1,1-dimethyl-6-tert-butylindan (ADBI, or Celestolide®), 6-acetyl-1,1,2,3,3,5-hexamethylindan (AHMI, or Phantolide®), 5-acetyl-1,1,2,6-tetramethyl-3-isopropylindane (ATII, or Traesolide®) and two nitromusks: 1-tert-butyl-3,5-dimethyl-2,4,6-trinitrobenzene (musk xylene) and 4-acetyl-1-tert-butyl-3,5-dimethyl-2,6-dinitrobenzene (musk ketone). This was done using an Agilent 6890 gas chromatograph (GC) with a J&W Scientific DB-5 MS fused silica capillary column (30 m x 0.25 mm I.D.) with the injection port set to 275 ºC and helium flow set to 1.9 mL/min, coupled to an Agilent 5973 mass spectrometric detector (MSD) in electron ionization (EI) mode with ion source at 230 ºC, quadrupole at 150 ºC, and transfer line at 250 ºC. Concentrations were corrected for internal standard recoveries.

Quality Control. Every batch of PEs was extracted alongside a laboratory blank and two additional blanks extracted in solvent spiked with all target compounds. Spiked samples were

103 used to track losses during extraction, concentration, and cleanup. Average recoveries ranged
104 from 79% for musk xylene to 145% for musk ketone (Table S3). The relative percent
105 differences (RPD) between ambient concentrations from duplicate samplers are shown in Table
106 S4. For air PEs, the mean RPD was 18% for HHCB and 21% for AHTN (N=18). For water
107 PEs, the mean RPD was 15% for HHCB and 25% for AHTN (N= 14).

108 Field blanks were sent to each volunteer along with PEs intended for deployment. Field
109 blanks were transported to the sampling site along with other PEs, taken out of their packaging,
110 handled by the volunteer, and then immediately re-packaged and shipped back to the laboratory
111 for analysis. Concentrations of target compounds in deployed PEs were blank-subtracted using
112 the most relevant field blank. For offshore deployments done from research vessels, all field
113 blanks taken during the cruise were averaged and the average field blank value was subtracted
114 from all samples collected.

115 After blank subtraction, the detection limit (DL) in ng/g PE was defined as twice the
116 standard deviation for all 11 laboratory blanks, as these samples were representative of the
117 typical variability in background concentrations in the laboratory. Concentrations below
118 detection limits were replaced with zero. Average blank concentrations and detection limits per
119 gram polyethylene are shown in Table S5. For HHCB, which was typically found at greatest
120 concentrations in the blanks, average blank concentrations were 13 ng/g PE, 28 ng/g PE, and 4
121 ng/g PE in laboratory blanks, shoreline volunteer field blanks, and shipboard field blanks,
122 respectively.

123 To better describe the detection limits for PEs, typical DLs in ng/g PE were translated to
124 air and water concentrations using the average percent equilibration for each site type and

assuming an average temperature of 18.85 ºC for summer deployments and 4.85 ºC for winter deployments (Table S6). For air samples, typical ambient detection limits were about 0.9 ng/m^3 for HHCB and 0.07 ng/m^3 for AHTN at summer shoreline and offshore sites, and 0.2 ng/m^3 for HHCB and 0.01 ng/m^3 for AHTN at winter shoreline sites. In water samples, typical detection limits were about 0.6 ng/L for HHCB and 0.04 ng/L for AHTN, with no significant difference between offshore and shoreline samples. Actual detection limits varied from site to site depending on the PE's sampling rate, and all blank subtraction was done using concentrations per weight of polyethylene, before conversion to ambient air and water concentrations.

Percent detection for target compounds is presented in Table S7. HHCB and AHTN were found in 15% and 68% of all shoreline air PEs deployed in this study and in 38% and 54% of offshore/nearshore air PEs. In water, HHCB and AHTN were found in 45% and 60% of shoreline water PEs and in 47% and 79% of offshore water PEs.

Physico-chemical Properties. Physico-chemical properties of all target analytes and PRCs are presented in Table S8. PE-air partitioning coefficients (K_{PEA}) were determined from regression with sub-cooled liquid vapor pressure as in Khairy and Lohmann.[15] PE-water partitioning coefficients (K_{PEW}) were calculated from solubility as in Lohmann.[21] K_{PEA}, K_{PEW}, and diffusivity in air (D_a) and water (D_w) for each compound were corrected for each deployment's mean temperature, as detailed further in the SI.

Sampling Rates and Ambient Concentrations. To determine ambient concentration (C_a), the concentration in the PE (C_{PE}) was adjusted for the percent equilibration (*f*) reached during deployment as in Equation 1. A detailed summary of these calculations is presented in the SI. Briefly, percent loss of each PRC (1-*f*) was plugged into a generalized exponential model for PE

uptake (Equation 2) to derive a best-fit value for the thickness of the diffusive boundary layer (δ_{DBL}) using a nonlinear least-squares fitting method adapted from Booij et al.[22] In Equation 2, t is total deployment time (listed for each deployment in Table S1), l_{PE} is half the PE thickness, K_{PEM} is the PE-matrix partitioning coefficient, and k_o is the mass transfer coefficient, which represents the reciprocal sum of PE-side resistance (k_{PE}^{-1}), which is dependent on D_{PE} and l_{PE}, and environmental matrix-side resistance (k_m^{-1}), which is dependent on D_a or D_w and δ_{DBL}. Best-fit δ_{DBL} values were used to estimate f reached by each PCM during each deployment.

$$C_a = \frac{C_{PE}}{K_{PEA} \cdot f} \quad (1)$$

$$f = 1 - e^{\frac{-t \cdot k_0 \cdot A_{PE}}{K_{PEM} \cdot V_{PE}}} \quad (2)$$

Average f values for each PCM are presented in Table S9 and show that HHCB and AHTN generally reached $\geq$ 95% equilibrium in both air and water. Average δ_{DBL}s for air boundary layers (δ_{ABL}) were lower for offshore/nearshore PEs (0.2±0.1 mm; average ±stdev) than for shoreline PEs (1.8±1.4 mm in summer and 1.4±0.5 mm in winter). This translated to average HHCB sampling rates of 5.7±0.9 m^3/day for winter PEs, 6.9±2.3 m^3/day for shoreline summer PEs, and 13±0.9 m^3/day for offshore PEs. Average water boundary layer thickness (δ_{WBL}) was 170±63 µm at shoreline sites and 82±25 µm at offshore sites, which translated to average sampling rates for HHCB of 16±3.8 L/day for shoreline PEs and 9.2±4.1 L/day for offshore PEs.

Best-fit δ_{DBL} and other compound-specific and site-specific parameters were plugged into the equation for f to determine typical equilibration times for the PCMs measured in this study. HHCB and AHTN tended to equilibrate within about 25 days in water and 19 days in air, so mean concentrations were representative of these time lengths, though PEs were often deployed for longer. Use of thicker polyethylene sheeting in future deployments would allow for time-integrated concentrations of HHCB and AHTN to be measured over longer time periods.

Data Analysis and Statistical Methods. Human population data was extracted from the Global Rural-Urban Mapping Project (GRUMP) Population Count Grid dataset provided by Columbia University[23] and maps were constructed in ArcMap for Desktop 10.3.1. To find the radii at which population and Σ_5PCM correlated most strongly, the model with the lowest residual standard error (RSE) was identified using the ordinary least-squares linear modeling function (*lm*) in R.[24] Linear models were further refined using the robust linear model (*rlm*) function in the MASS package in R,[25] which iteratively fits data to a linear model, weighting outliers depending on their distance from the best-fit line. All presented relationships were found to be statistically significant ($p < 0.01$) using both approaches. Results were plotted using R package *ggplot2*.[26]

Air-Water Exchange Calculations. 32 pairs of co-deployed air and water PEs were used to investigate time-integrated air-water exchange fluxes. The direction of exchange was determined by calculating the ratio of fugacity in water to fugacity in air (f_w/f_a) as in Equation 3, where $C_{\infty,w}$ and $C_{\infty,a}$ represent the concentration of the compound in the PE once it has reached equilibrium with surrounding water and air, respectively.

$$\frac{f_w}{f_a} = \frac{C_{\infty,w}}{C_{\infty,a}} \quad (3)$$

$f_w/f_a > 1$ indicates volatilization while $f_w/f_a < 1$ indicates absorption. In cases where the concentration in both air and water were <DL, no fugacity ratio was calculated. In cases where the concentration in one medium was <DL, but was >DL in the other medium, a fugacity ratio was calculated by replacing the <DL value with the DL value, as this resulted in the most conservative estimate for the fugacity ratio (see Figure S2).

$C_{\infty,w}$ and $C_{\infty,a}$ were determined by correcting the concentration in the PE (C_{PE}) using the calculated percent equilibrium (f) reached by each compound during deployment. In most cases for AHTN and HHCB, $C_\infty \sim C_{PE}$ because they equilibrated during deployment. The uncertainty in the fugacity ratio was calculated by propagating the uncertainty in the parameters used to calculate $C_{\infty,a}$ and $C_{\infty,w}$, which is detailed further in the SI. In cases where the fugacity ratio was within one standard deviation from equilibrium, it was not considered significantly different from equilibrium and no flux was calculated.

Air-water exchange fluxes ($F_{a/w}$) were calculated using an approach based on the Whitman two-film model[27] as described in Schwarzenbach et al.[28] with wind speed's effect on water-side mass transfer determined using a Weibull distribution to account for the non-linearity of the effect of wind speed on mass transfer.[29] The mass transfer coefficient ($v_{a/w}$) was multiplied by the concentration gradient as in Equation 4, where $K_{PEW,T2}$ is the PE-water partitioning coefficient corrected for deployment temperature. Similar approaches have previously been used to estimate air-water exchange fluxes from PE pairs for polychlorinated biphenyls (PCBs), polybrominated diphenyl ethers (PBDEs), and polycyclic aromatic

hydrocarbons (PAHs) in the Great Lakes,[20,17,30] but PCMs have not been investigated. Uncertainty in exchange fluxes was calculated using the uncertainty of the parameters used to calculate $C_{\infty,a}$, $C_{\infty,w}$, and $K_{PEW,T2}$, and assuming 30% relative uncertainty in $v_{a/w}$.[31] Calculations and error propagation are detailed further in the SI.

$$F_{a/w} = v_{a/w} \cdot \frac{(C_{\infty,w} - C_{\infty,a})}{K_{PEW,T2}} \quad (4)$$

RESULTS AND DISCUSSION

Dissolved PCM Concentrations. Average dissolved Σ_5PCM ranged from <DL at Cape Vincent (CV) in eastern Lake Ontario to 2.6 ng/L near the mouth of the Oswego River (OSW) on the southern shoreline of Lake Ontario. Average dissolved concentrations of AHTN and HHCB are shown in Figure 1A.

Average dissolved PCMs are summarized in Table 1. Along the southeastern shore of Lake Erie and the northeastern shore of Lake Ontario, concentrations were similar to offshore levels (Σ_5PCM < 100 pg/L) and HHCB was generally <DL, while concentrations were elevated nearer to the urban centers of Toronto and Cleveland and along the southern shore of Lake Ontario. Variation in dissolved Σ_5PCM over multiple deployments is shown in Figure S3.

Overall, concentrations reported from PEs were similar but lower than previous results: Peck and Hornbuckle measured PCMs in Lake Michigan in 1999-2000 using shipboard active sampling with XAD-2 resin and reported means of 5 ng/L for HHCB and 1 ng/L for AHTN.[4]

227 Helm et al. estimated concentrations of 0.2 – 10 ng/L and 0.1 – 10 ng/L for HHCB and AHTN,
228 respectively, east of Toronto in June 2008 using semi-permeable membrane devices (SPMDs).[32]
229 In offshore Lake Ontario, Andresen et al. measured HHCB and AHTN by liquid-liquid
230 extraction of water samples at 2.0 ng/L and 0.2 ng/L, with concentrations increasing to 7.0 ng/L
231 for HHCB and 0.8 ng/L for AHTN in Hamilton Harbor.[33] Concentrations in this study were
232 typically lower than in urban creeks near Toronto (2-1000 ng/L, with lower concentrations (0.04
233 – 18 ng/L) in the less populated Rouge River watershed).[5] This was expected, as the sites
234 monitored in this study were not as directly representative of upriver source regions.

235 At sites where both HHCB and AHTN were detected, the ratio of HHCB:AHTN ranged
236 from 7-12, with an average of 10±2, which was similar to that reported by Buerge et al. for
237 summertime surface waters in a Swiss lake (HHCB:AHTN 6 – 9) and by Andresen et al. in Lake
238 Ontario in 2005 (~ 10).[33,34] HHCB:AHTN ratios were, in most cases, greater than those
239 measured in source region studies. Buerge et al. estimated that the half-life of HHCB with
240 respect to photolysis in water was about 25 times longer than for AHTN, so increasing
241 HHCB:AHTN ratio in water with distance from source was expected.[34]

242 Nitromusks were not found above a 3:1 signal:noise level in the majority of water
243 samples and were therefore omitted from discussion. Previous studies generally found musk
244 xylene and musk ketone at levels near or below this study's typical detection limits (19 pg/L for
245 musk xylene and 225 pg/L for musk ketone). Peck and Hornbuckle found median concentrations
246 in Lake Michigan of 49 pg/L for musk xylene and 81 pg/L for musk ketone, and Andresen et al.
247 measured both nitromusks at about 40 pg/L in Hamilton Harbor, Lake Ontario.[4,33]

Gaseous PCM Concentrations. Average summertime Σ_5PCM ranged from <DL at sites in Erie (ERI) and Sheffield Lake (SHF) on the southern Lake Erie shoreline, Prince Edward Point (PEP) in northern nearshore Lake Ontario, and eastern offshore Lake Erie (EERI), to 3.2 ng/m^3 in Toledo (TOL). Concentrations of all gaseous PCMs are summarized in Table 2. Average summertime HHCB and AHTN concentrations are displayed in Figure 1B. Summertime concentrations were lowest at offshore buoy sites (< 300 pg/m^3, with HHCB <DL), with the exception of three buoy sites near the Toronto waterfront, where concentrations were comparable to or greater than shoreline sites. Concentrations at shoreline sites were generally greater in the summer than in the winter. Variations in Σ_5PCM over multiple deployments are depicted in Figure S4.

A possible explanation for the low incidence of detection of HHCB in this study is its short atmospheric lifetime (about 5.3 hours) with respect to photolysis.[35] HHCB:AHTN ratios in air have previously been shown to decrease with distance from source regions, suggesting that gaseous HHCB may degrade more rapidly than AHTN.[36] At sites where both AHTN and HHCB were >DL, the average HHCB:AHTN ratio ranged from 3.8 in eastern nearshore Toronto (ETOR) to 6.6 in Toledo (TOL), with an average value of 5±1, somewhat similar to ratios measured by Xie et al. in rural Germany (median 3.5).[36]

PCMs are relatively volatile (0.02 - 1.2 Pa)[4] compared to other semi-volatile organic contaminants (SVOCs) and a significant fraction of these compounds (> 80%) is typically found in the gaseous phase, suggesting that PE-derived concentrations should match those from other air sampling techniques. Indeed, results from previous studies were similar: Peck and Hornbuckle measured gas-phase PCMs in 1999-2001 using XAD-2 resin throughout the Great

Lakes and found average urban $\sum_2$PCM (AHTN + HHCB) around 1-5 ng/m^3 with mean offshore Lake Erie and Lake Ontario concentrations <0.5 ng/m^3.[37] Furthermore, average $\sum_2$PCM concentrations in Toronto nearshore air measured in this study (1.6- 3.1 ng/m^3) were comparable to those measured by Melymuk et al. during 2007-2008 using polyurethane foam (PUF) samplers within 10 km of the Toronto central business district (0.89-3.5 ng/m^3).[38]

As in water, the nitromusks were not found above 3:1 signal:noise levels in the majority of air samples and were therefore omitted from discussion. In previous work by Peck and Hornbuckle in the lower Great Lakes region, nitromusks in air were found above method reporting limits only intermittently and at levels under 80 pg/m^3.[37]

Correlation of PCM concentrations with Population Density. Previous studies have identified population centers as sources of gaseous PCMs to ambient air[37] and have shown correlations between population density and PCMs in air and water.[34,39,40] To investigate the relationship between PCMs and population density in the lower Great Lakes, average summertime concentrations were compared to population within 2 to 50 km of each site. The strongest correlations found for gaseous and dissolved PCMs are displayed in Figure 2.

Gaseous Σ_5PCM exhibited significant ($p < 0.01$) correlation with population within a 15-50 km radius of each site. The correlation was strongest when considering population within 25 km ($p < 0.001$; SE = 0.33; N = 22). The two locations with the greatest residuals were Toledo (TOL) and Cleveland Edgewater (CLE), both of which exhibited greater gaseous Σ_5PCM than would be predicted from population based on the presented regression. This suggests elevated concentrations in these areas may be caused by nearby point sources not representative of the surrounding region.

Dissolved Σ_5PCM exhibited significant ($p < 0.01$) correlation with population within a 20-40 km radius of each site, with the strongest correlation observed when considering population within 40 km ($p < 0.005$; SE = 0.26; N = 20). The strong correlation at such a large radius may be because spatial distributions are influenced by wastewater outfalls and river mouths, both of which are point sources that represent a much larger area's population (the watershed). Concentrations near the mouth of Oswego River exhibited the greatest residuals, again suggesting a nearby point source.

River and Wastewater Discharge. Dissolved PCMs were elevated at many shoreline sites impacted by nearby WWTPs designated as major dischargers by the US Environmental Protection Agency (EPA) National Pollutant Discharge Elimination System (NPDES),[41] many of which discharged directly into the lakes. More details on sites with elevated concentrations and possible sources are included in the SI.

Air-Water Exchange. ***Fugacity Ratios.*** Fugacity ratios for all air-water PE pairs are displayed in Table S10 and depicted in Figure S2. At all sites where HHCB was detected in air and/or water, fugacity ratios suggested it was volatilizing out of surface waters. Fugacity ratios for AHTN also suggested volatilization from surface waters near Toronto and along the southern shore of Lake Ontario, though AHTN was near equilibrium or absorbed into surface waters at some other sites.

The greatest fugacity ratios for both AHTN (f_w/f_a = 7) and HHCB (f_w/f_a = 18) were calculated for the PE pair from the late-summer deployment near the mouth of the Oswego River (OSW), during which greater dissolved PCMs were measured than during any other deployment (Σ_5PCM = 4.8 ng/L). Fugacity ratios were generally not significantly different from equilibrium

314 at sites on the southeastern shore of Lake Erie (ERI, DUN, BUF), the northeastern Lake Ontario
315 shoreline/nearshore (CV, PEP, CHB), or at the offshore sites (CERI, EERI).

316 ***PE-Derived Air-Water Exchange Fluxes at Non-Steady-State Conditions.*** Values of $v_{a/w}$
317 calculated for HHCB and AHTN ranged from 4.5-8.8 cm/day, which was somewhat slower than
318 rates for PCBs calculated by Liu et al. (15-63 cm/day) and within the range for 4-ring PAHs
319 calculated by McDonough et al. (1-16 cm/day).[20] These rates were used along with mass
320 transfer coefficients for PE uptake (k_o) of HHCB from air (181-6,905 cm/day) and water (14-47
321 cm/day) to determine how air-water exchange fluxes derived from co-deployed air and water
322 PEs compared to actual values in scenarios where concentrations in air and water are not at
323 steady state.

324 A model was written in R in which air and water concentrations of HHCB were set to
325 vary every 6 hours over 100 days. In Scenario 1, both air and water concentrations fluctuated
326 randomly between minimum and maximum values based on realistic concentration ranges from
327 this and previous studies (1-6 ng/m^3 in air; 0.5-8 ng/L in water). In Scenario 2, air
328 concentrations fluctuated randomly around a steadily increasing mean from 5 to 12 ng/m^3 and
329 water concentrations declined from 6 to 1 ng/L, also with random fluctuations, resulting in a
330 reversal of the flux direction during the deployment. The air-water exchange flux (F_{aw}) at each
331 time point was calculated from the simulated air and water concentrations at that time.

332 At each time point, the mass of HHCB accumulated in air and water PEs in response to
333 the fluctuating ambient concentrations was computed, and the PE-derived air-water exchange
334 flux ($F_{aw,PE}$) was calculated based on the concentrations of HHCB in the co-deployed PEs at that
335 time. F_{aw} was then compared to $F_{aw,PE}$ by calculating the RPD between the two values. An

example from Scenario 2, in which F_{aw} decreased throughout the simulated deployment, is displayed in Figure 3. $F_{aw,PE}$ is shown to steadily decline over the deployment along with F_{aw}, but $F_{aw,PE}$ does not capture rapid day-to-day changes in the flux and appears to lag behind F_{aw} by about 20 days. A similar figure is shown for Scenario 1 in Figure S5.

Each scenario was run 100 times, and each time the RPD between $F_{aw,PE}$ and F_{aw} after 100 days of deployment was recorded. Results are presented in Table 3 as the mean RPD between $F_{aw,PE}$ and three values: F_{aw} on the last day of the simulated deployment (Day 100), the average F_{aw} over the typical equilibration time for HHCB (defined as 22 days, the average of air and water PE equilibrium times), and the average F_{aw} over the entire 100-day deployment. Results show that PE-derived exchange fluxes provide a good estimate of mean F_{aw} over the last 22 days in both scenarios, though they were not always representative of instantaneous fluxes the day they were recovered, or of average fluxes over the entire deployment period.

Table 3 also shows RPDs determined by comparison of "actual" fluxes (F_{aw}) and fluxes that would be derived from weekly grab samples . Grab samples were simulated by taking values of the "actual" concentrations of PCMs in air and water once a week, calculating instantaneous exchange fluxes, and averaging these values over the 100-day deployment, or over the last 22 days. Results suggest that $F_{aw,PE}$ is more representative of the mean F_{aw} over the last 22 days than taking 3 weekly grab samples, while weekly grab samples are more appropriate for capturing mean flux over 100 days in cases where the exchange flux changes steadily over time, as in Scenario 2. In summary, PEs resulted in a very good approximation of the actual air-water exchange flux during the compounds' equilibration time window, in some cases superior to weekly grab sampling.

PCM Air-Water Exchange Fluxes. Air-water exchange mass transfer coefficients and exchange fluxes for all PE pairs with fugacity ratios significantly different from equilibrium are provided in Tables S11 and S12. Figure 4 shows air-water exchange fluxes calculated for HHCB and AHTN in ng/m^2/day during each deployment for which data was available. As demonstrated in the previous section, these fluxes were representative of time-averaged air-water exchange fluxes over the last 3 weeks prior to sampler recovery.

Volatilization fluxes of HHCB and AHTN ranged from 11±6 ng/m^2/day and -3±2 ng/m^2/day during the first deployment near the shore of Cleveland, OH (CLE) to 341±127 ng/m^2/day and 28±10 ng/m^2/day during late summer near the mouth of Oswego River (OSW). Few previous measurements of PCM air-water exchange fluxes are available for comparison. Xie et al. measured median net air-water volatilization of 27 ng/m^2/day and 14 ng/m^2/day for HHCB and AHTN in the North Sea, and measured net deposition of both compounds in the Arctic.[36]

IMPLICATIONS

Results from this study suggest that WWTPs may be responsible for influencing spatial distributions of dissolved PCMs in the lower Great Lakes, and that PCMs in the lakes were volatilizing from surface waters at many locations near urbanized shorelines. Previous studies of the Great Lakes region have estimated that volatilization is an important loss route for dissolved PCMs. Melymuk et al. estimated that volatilization removes 31% of total inputs of PCMs from the Toronto area, about 210±120 kg/yr, from Lake Ontario.[5] Peck and Hornbuckle estimated that volatilization was responsible for the loss of about 290 kg/yr of PCMs from Lake Michigan.[4]

Volatilization fluxes in this study were driven by elevated dissolved concentrations at shoreline and nearshore sites. These elevated concentrations were expected to be entrained in the nearshore coastal boundary zone, which extends from the shoreline to where the depth of the lake exceeds that of the thermocline.[42] To estimate total losses of dissolved PCMs from the lakes via volatilization, fluxes were averaged over the estimated surface area of the urbanized coastal boundary zone.

The surface area of the Lake Ontario coastal boundary zone was estimated to be 6500 km^2 by extracting the area with depth shallower than 50 meters using GIS data from the Great Lakes Commission's Great Lakes Information Network (GLIN), as shown in Figure S6. The coastal boundary zone in Lake Erie was more difficult to define, as most of the lake is quite shallow and it does not develop a pronounced seasonal thermocline as in Lake Ontario. From GLIN data, the surface area of Lake Erie shallower than 20 m was estimated to be 15200 km^2.

Averaging fluxes at all Lake Ontario sites yielded a mean Σ_5PCM flux of 58 $ng/m^2/day$ over the coastal boundary zone. Assuming fluxes of this magnitude occurred over 30%–100% the total coastal boundary zone and that fluxes of this magnitude occur all year long, we estimated that 41-138 kg/year Σ_5PCM could be lost to volatilization in Lake Ontario. Lake Erie data yielded an average Σ_5PCM flux of 13 $ng/m^2/day$, suggesting that 22-74 kg/year Σ_5PCM could be lost to volatilization in Lake Erie. This may be an overestimate, as fluxes could be lower in the winter, when the surface waters freeze and lower temperatures drive down PCM vapor pressure, but the absence of wintertime dissolved concentration data prohibited flux calculations for these months. While these estimations are based on temporally- and spatially-limited data, they are of a similar magnitude to those estimated in previous Great Lakes studies,

and suggest that volatilization may be a significant loss process for dissolved PCMs in this region.

ASSOCIATED CONTENT

Supporting Information. Additional figures and tables are available in the Supporting Information along with explanations of calculations to derive percent equilibration and propagate uncertainty in fugacity ratios. This material is available free of charge via the Internet at http://pubs.acs.org.

AUTHOR INFORMATION

Corresponding Author

* Rainer Lohmann: rlohmann@uri.edu

Author Contributions

The manuscript was written through contributions of all authors. All authors have given approval to the final version of the manuscript.

ACKNOWLEDGMENTS

We would like to acknowledge funding from the US EPA Great Lakes Restoration Initiative (GLRI) GLAS #00E00597-0, project officer Todd Nettesheim. We would also like to express our gratitude to Professor Peter August (URI) for assistance with GIS analysis, David Adelman (URI) for sampler preparation and field deployment logistics, Camilla Teixeira and the field staff of the Emergencies, Operational Analytical Laboratories, and Research Support group

(Environment Canada Burlington) for open-lake PE deployments, Great Lakes Unit field staff of the Ontario Ministry of the Environment and Climate Change for Lake Ontario nearshore deployments, and all of the volunteers who deployed PEs throughout the Great Lakes region.

441

442 **REFERENCES**

443 (1) Rimkus, G. G. Polycyclic musk fragrances in the aquatic environment. *Toxicol. Lett.*
444 **1999**, *111*, 37–56, DOI:10.1016/S0378-4274(99)00191-5.

445 (2) Hornbuckle, K.; Peck, A. M. Environmental Sources, Occurrence, and Effects of
446 Synthetic Musk Fragrances. *J. Environ. Monit.* **2006**, *8*, 874–879, DOI:10.1039/b608170n.

447 (3) Homem, V.; Silva, J. A.; Ratola, N.; Santos, L.; Alves, A. Long lasting perfume--a review
448 of synthetic musks in WWTPs. *J. Environ. Manage.* **2015**, *149*, 168–192,
449 DOI:10.1016/j.jenvman.2014.10.008.

450 (4) Peck, A. M.; Hornbuckle, K. C. Synthetic musk fragrances in Lake Michigan. *Environ.*
451 *Sci. Technol.* **2004**, *38*, 367–372, DOI:10.1021/es034769y.

452 (5) Melymuk, L.; Robson, M.; Csiszar, S. A.; Helm, P. A.; Kaltenecker, G.; Backus, S.;
453 Bradley, L.; Gilbert, B.; Blanchard, P.; Jantunen, L.; Diamond, M. L. From the city to the
454 Lake: loadings of PCBs, PBDEs, PAHs and PCMs from Toronto to Lake Ontario.
455 *Environ. Sci. Technol.* **2014**, *48*, 3732–3741, DOI:10.1021/es403209z.

456 (6) Bester, K. Polycyclic musks in the Ruhr catchment area--transport, discharges of waste
457 water, and transformations of HHCB, AHTN and HHCB-lactone. *J. Environ. Monit.* **2005**,
458 *7*, 43–51, DOI:10.1039/b409213a.

459 (7) Howard, P. H.; Muir, D. C. G. Identifying New Persistent and Bioaccumulative Organics
460 Among Chemicals in Commerce. *Environ. Sci. Technol.* **2010**, *44*, 2277–2285,
461 DOI:10.1021/es903383a.

462 (8) Gatermann, R.; Biselli, S.; Hühnerfuss, H.; Rimkus, G. G.; Hecker, M.; Karbe, L.
463 Synthetic musks in the environment. Part 1: Species-dependent bioaccumulation of
464 polycyclic and nitro musk fragrances in freshwater fish and mussels. *Arch. Environ.*
465 *Contam. Toxicol.* **2002**, *42*, 437–446, DOI:10.1007/s00244-001-0041-2.

466 (9) O'Toole, S. O.; Metcalfe, C. Synthetic Musks in Fish from Urbanized Areas of the Lower
467 Great Lakes , Canada. *J. Gt. Lakes Res.* **2006**, *32*, 361–369, DOI:10.3394/0380-
468 1330(2006)32[361:SMIFFU]2.0.CO;2.

469 (10) Reiner, J. L.; Kannan, K. Polycyclic Musks in Water, Sediment, and Fishes from the
470 Upper Hudson River, New York, USA. *Water, Air, Soil Pollut.* **2010**, *214*, 335–342,
471 DOI:10.1007/s11270-010-0427-8.

472 (11) Parolini, M.; Magni, S.; Traversi, I.; Villa, S.; Finizio, A.; Binelli, A. Environmentally
473 relevant concentrations of galaxolide (HHCB) and tonalide (AHTN) induced oxidative
474 and genetic damage in Dreissena polymorpha. *J. Hazard. Mater.* **2015**, *285*, 1–10,
475 DOI:10.1016/j.jhazmat.2014.11.037.

476 (12) Lohmann, R.; Muir, D. Global Aquatic Passive Sampling (AQUA-GAPS): using passive
477 samplers to monitor POPs in the waters of the world. *Environ. Sci. Technol.* **2010**, *44*,
478 860–864, DOI:10.1021/es902379g.

479 (13) Adams, R. G.; Lohmann, R.; Fernandez, L. A.; Macfarlane, J. K.; Gschwend, P. M.

Polyethylene Devices: Passive Samplers for Measuring Dissolved Hydrophobic Organic Compounds in Aquatic Environments. *Environ. Sci. Technol.* **2007**, *41*, 1317–1323, DOI:10.1021/es0621593.

(14) Lohmann, R.; Booij, K.; Smedes, F.; Vrana, B. Use of passive sampling devices for monitoring and compliance checking of POP concentrations in water. *Environ. Sci. Pollut. Res. Int.* **2012**, *19*, 1885–1895, DOI:10.1007/s11356-012-0748-9.

(15) Khairy, M. A.; Lohmann, R. Field calibration of low density polyethylene passive samplers for gaseous POPs. *Environ. Sci. Process. Impacts* **2014**, *16*, 414–421, DOI:10.1039/c3em00493g.

(16) Bartkow, M. E.; Booij, K.; Kennedy, K. E.; Müller, J. F.; Hawker, D. W. Passive air sampling theory for semivolatile organic compounds. *Chemosphere* **2005**, *60*, 170–176, DOI:10.1016/j.chemosphere.2004.12.033.

(17) McDonough, C. A.; Khairy, M. A.; Muir, D. C. G.; Lohmann, R. Significance of population centers as sources of gaseous and dissolved PAHs in the lower Great Lakes. *Environ. Sci. Technol.* **2014**, *48*, 7789–7797, DOI:10.1021/es501074r.

(18) Khairy, M.; Muir, D.; Teixeira, C.; Lohmann, R. Spatial Trends, Sources, and Air–Water Exchange of Organochlorine Pesticides in the Great Lakes Basin Using Low Density Polyethylene Passive Samplers. *Environ. Sci. Technol.* **2014**, *48*, 9315–9324, DOI:10.1021/es501686a.

(19) Tidwell, L. G.; Allan, S. E.; Connell, S. G. O.; Hobbie, K. A.; Smith, B. W.; Kim, A. PAH and OPAH Air and Water Exchange during the Deepwater Horizon Incident. *Environ. Sci. Technol.* **2016**, *50*, 7489–7497, DOI:10.1021/acs.est.6b02784.

(20) Liu, Y.; Wang, S.; McDonough, C. A.; Khairy, M.; Muir, D. C. G.; Helm, P. A.; Lohmann, R. Gaseous and freely-dissolved PCBs in the lower Great Lakes based on passive sampling: spatial trends and air-water exchange. *Environ. Sci. Technol.* **2016**, *50*, 4932–4939, DOI:10.1021/acs.est.5b04586.

(21) Lohmann, R. Critical review of low-density polyethylene's partitioning and diffusion coefficients for trace organic contaminants and implications for its use as a passive sampler. *Environ. Sci. Technol.* **2012**, *46*, 606–618, DOI:10.1021/es202702y.

(22) Booij, K.; Smedes, F. An Improved Method for Estimating in Situ Sampling Rates of Nonpolar Passive Samplers. *Environ. Sci. Technol.* **2010**, *44*, 6789–6794, DOI:10.1021/es101321v.

(23) Center for International Earth Science Information Network (CIEISIN); Columbia University; International Food Policy Research Institute (IFPRI); The World Bank; Centro Internacional de Agricultura Tropical (CIAT). Global Rural-Urban Mapping Project, Version 1 (GRUMPv1): Population Count Grid http://sedac.ciesin.columbia.edu/data/set/grump-v1-population-count.

(24) R Core Team. R: A language and environment for statistical computing (version 3.1.0), 2014.

(25) Venables, W. N.; Ripley, B. D. *Modern Applied Statistics with S. Fourth Edition.*; Springer: New York, New York, USA, 2002.

(26) Wickham, H. *ggplot2: Elegant Graphics for Data Analysis*; Springer-Verlag: New York, New York, USA, 2009.

(27) Whitman, W. G. A Preliminary Experimental Confirmation of the Two-Film Theory of Gas Absorption. *Chem. Metall. Eng.* **1923**, *29*, 146–148, DOI:10.1016/0017-9310(62)90032-7.

(28) Schwarzenbach, R. P.; Gschwend, P. M.; Imboden, D. M. *Environmental Organic Chemistry*; 2nd ed.; Wiley Interscience, 2002.

(29) Zhang, H.; Eisenreich, S. J.; Franz, T. R.; Baker, J. E.; Offenberg, J. H. Evidence for Increased Gaseous PCB Fluxes to Lake Michigan from Chicago. *Environ. Sci. Technol.* **1999**, *33*, 2129–2137, DOI:10.1021/es981073+.

(30) Ruge, Z.; Muir, D.; Helm, P.; Lohmann, R. Concentrations, trends, and air-water exchange of PAHs and PBDEs derived from passive samplers in Lake Superior in 2011. *Environ. Sci. Technol.* **2015**, *49*, 13777–13786, DOI:10.1021/acs.est.5b02611.

(31) Rowe, M. D.; Perlinger, J. A. Micrometeorological measurement of hexachlorobenzene and polychlorinated biphenyl compound air-water gas exchange in Lake Superior and comparison to model predictions. *Atmos. Chem. Phys.* **2012**, *12*, 4607–4617, DOI:10.5194/acp-12-4607-2012.

(32) Helm, P. A.; Howell, E. T.; Li, H.; L. Metcalfe, T.; M. Chomicki, K.; D. Metcalfe, C. Influence of nearshore dynamics on the distribution of organic wastewater-associated chemicals in Lake Ontario determined using passive samplers. *J. Great Lakes Res.* **2012**, *38*, 105–115, DOI:10.1016/j.jglr.2012.01.005.

(33) Andresen, J. A.; Muir, D.; Ueno, D.; Darling, C.; Theobald, N.; Bester, K. Emerging pollutants in the North Sea in comparison to Lake Ontario, Canada, data. *Environ. Toxicol. Chem.* **2007**, *26*, 1081–1089, DOI:10.1897/06-416R.1.

(34) Buerge, I. J.; Buser, H.; Mu, M. D.; Poiger, T.; Wa, C. Behavior of the Polycyclic Musks HHCB and AHTN in Lakes, Two Potential Anthropogenic Markers for Domestic Wastewater in Surface Waters. *Environ. Sci. Technol.* **2003**, *37*, 5636–5644, DOI:10.1021/es0300721.

(35) Aschmann, S. M.; Arey, J.; Atkinson, R.; Simonich, S. L. Atmospheric lifetimes and fates of selected fragrance materials and volatile model compounds. *Environ. Sci. Technol.* **2001**, *35*, 3595–3600, DOI:10.1021/es010685i.

(36) Xie, Z.; Ebinghaus, R.; Temme, C.; Heemken, O.; Ruck, W. Air-sea exchange fluxes of synthetic polycyclic musks in the North Sea and the Arctic. *Environ. Sci. Technol.* **2007**, *41*, 5654–5659, DOI:10.1021/es0704434.

(37) Peck, A.; Hornbuckle, K. Synthetic musk fragrances in urban and rural air of Iowa and the Great Lakes. *Atmos. Environ.* **2006**, *40*, 6101–6111, DOI:10.1016/j.atmosenv.2006.05.058.

(38) Melymuk, L.; Robson, M.; Helm, P. A.; Diamond, M. L. PCBs, PBDEs, and PAHs in Toronto air: spatial and seasonal trends and implications for contaminant transport. *Sci. Total Environ.* **2012**, *429*, 272–280, DOI:10.1016/j.scitotenv.2012.04.022.

(39) Melymuk, L.; Robson, M.; Helm, P. A.; Diamond, M. L. Application of land use

regression to identify sources and assess spatial variation in urban SVOC concentrations. *Environ. Sci. Technol.* **2013**, *47*, 1887–1895, DOI:10.1021/es3043609.

(40) Lu, B.; Feng, Y.; Gao, P.; Zhang, Z.; Lin, N. Distribution and fate of synthetic musks in the Songhua River, Northeastern China: influence of environmental variables. *Environ. Sci. Pollut. Res. Int.* **2015**, *22*, 9090–9099, DOI:10.1007/s11356-014-3973-6.

(41) US EPA. US EPA Discharge Monitoring Report (DMR) Pollutant Loading Tool, v 1.0 https://cfpub.epa.gov/dmr/index.cfm.

(42) Rao, Y. R.; Schwab, D. J. Laurentian Great Lakes, Interaction of Coastal and Offshore Waters. *Encyclopedia of Lakes and Reservoirs*, 2012, 479–485.

585

586

587

588 **FIGURES AND TABLES**

589

590 **Table 1. Average dissolved PCMs (pg/L) summarized regionally**

	N [a]	ADBI	AHMI	ATII	HHCB	AHTN
Toronto Waterfront Nearshore	3	1.1 ± 0.7	2.2 ± 0.7	37 ± 6.6	1625 ± 242	162 ± 32
Southern L. Ontario Shoreline	3	1.2 ± 0.8	2.4 ± 1.3	28 ± 33	1363 ± 827	134 ± 66
Greater Cleveland Shoreline/Nearshore	3	1.5 ± 0.9	3.9 ± 2.2	29 ± 13	697 ± 222	72 ± 19
Southeast L. Erie Shoreline	3	0.1 ± 0.2	0.8 ± 0.3	3.0 ± 5.1	23 ± 39	16 ± 7.9
Northeast L. Ontario Nearshore	3	< DL	0.4 ± 0.4	2.1 ± 2.0	< DL	14 ± 12
Offshore L. Erie and L. Ontario	5	0.9 ± 1.2	2.5 ± 3.8	16 ± 21	< DL	28 ± 18

591 [a] N is the number of sites of each type.

592

593

594 **Table 2. Average gaseous PCMs (pg/m^3) grouped by site type**

	N [a]	ADBI	AHMI	ATII	HHCB	AHTN
Summer (May - November)						
Offshore/Nearshore Buoys	5	2.1 ± 4.6	2.2 ± 4.9	47 ± 106	< DL	5.4 ± 12
Toronto Waterfront Nearshore Buoys	3	0.6 ± 1.0	24 ± 17	493 ± 69	1529 ± 591	302 ± 88
L. Erie and L. Ontario Shoreline	14	2.8 ± 6.3	11 ± 9.5	100 ± 189	357 ± 836	149 ± 159
Winter (December - April)						
L. Erie and L. Ontario Shoreline	9	0.2 ± 0.6	0.8 ± 1.5	22 ± 44	29 ± 87	17 ± 19

595 [a] N is the number of sites of each type.

596

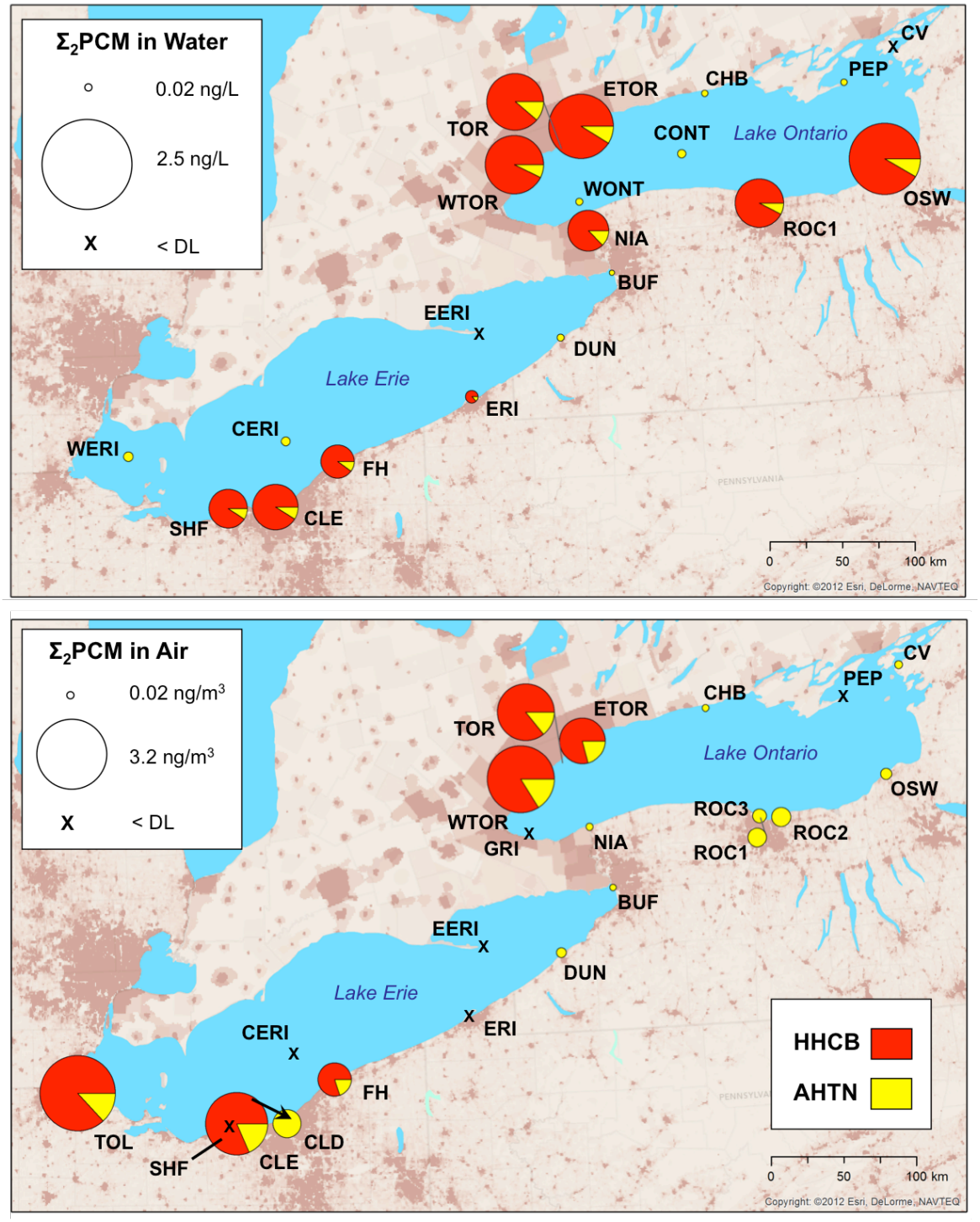

Figure 1. Average summer HHCB and AHTN (Σ_2PCM) concentrations throughout the lower Great Lakes. Average dissolved (top) and gaseous (bottom) HHCB and AHTN during summer deployments are shown with HHCB in red and AHTN in yellow. Gaseous Σ_2PCM ranged from <DL at sites marked by X's to 3.2 ng/m^3 in Toledo (TOL). Dissolved Σ_2PCM ranged from <DL at sites marked by X's to 2.5 ng/L near the mouth of Oswego River (OSW).

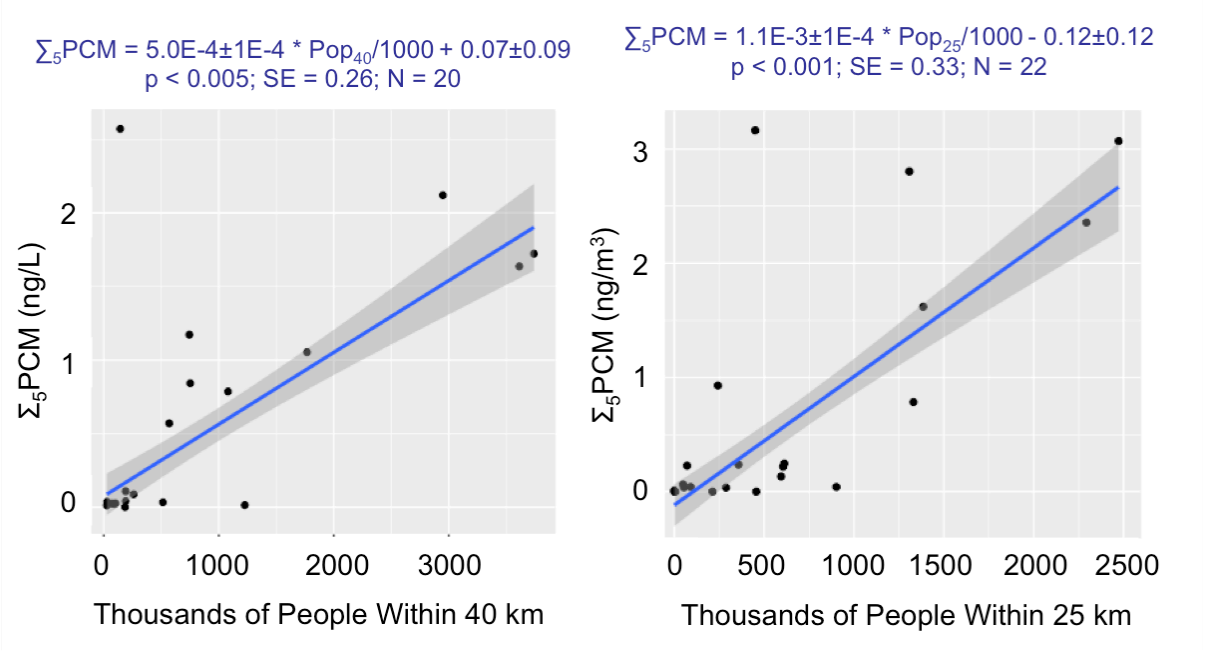

603

604 **Figure 2. Correlation of dissolved and gaseous Σ_5PCM and surrounding population**
605 **density.** Average summer dissolved (left) and gaseous (right) Σ_5PCM was most strongly
606 correlated with population within 25 km and 40 km of each site, respectively. 95% confidence
607 intervals for the linear models are shaded in gray.

608

609

610

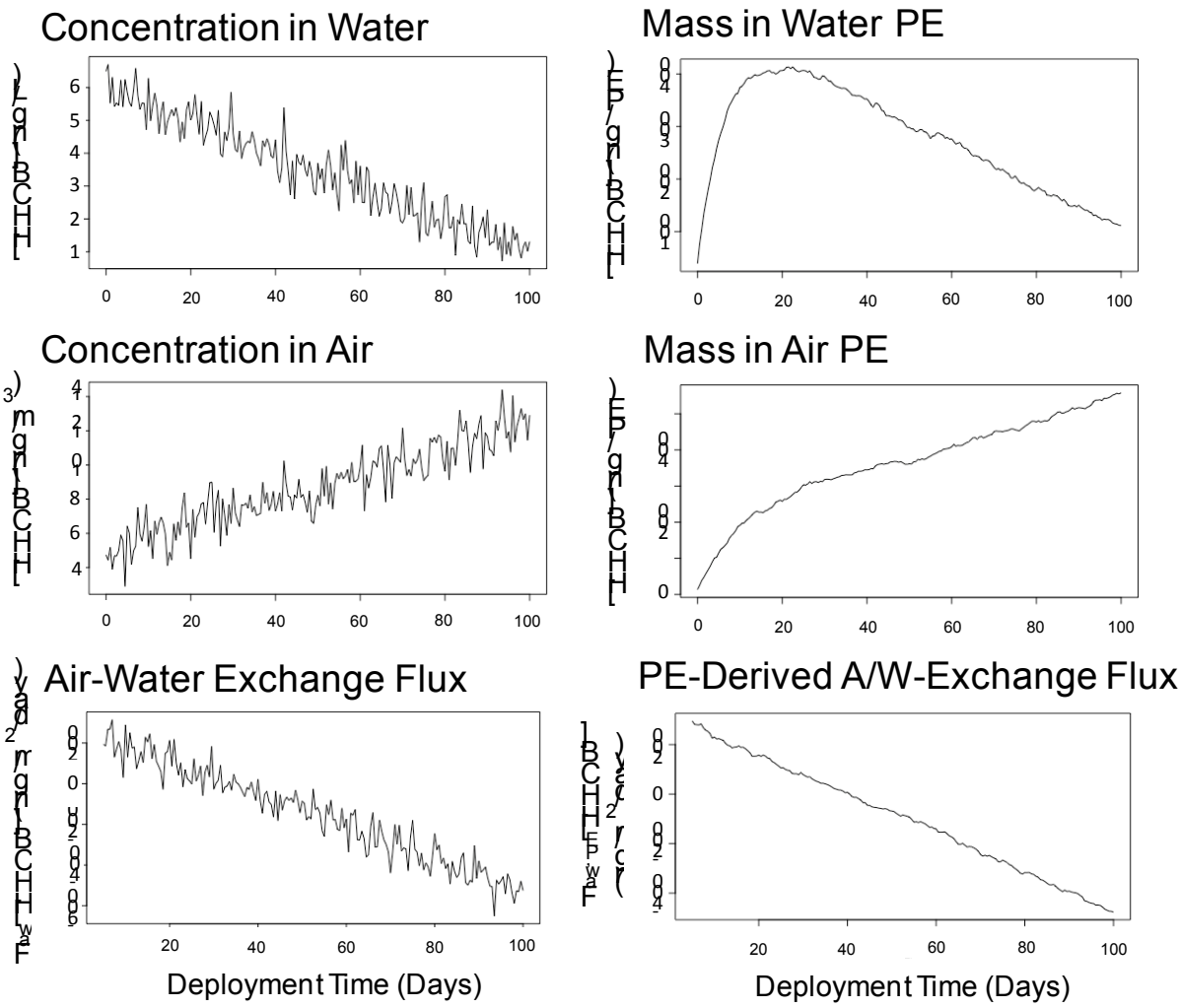

611

612 **Figure 3. Predicted Air-Water Exchange Fluxes Based on Simulated Air and Water HHCB**
613 **Concentrations.** Simulated water and air concentrations of HHCB and air-water exchange
614 fluxes calculated from these concentrations are shown on the left over a 100-day simulated
615 deployment. The mass of HHCB accumulated in a 2-gram PE in response to the simulated air
616 and water concentrations is shown on the left, along with the air-water exchange flux that would
617 be calculated using this pair of air and water PEs.

618

619

620

621

622

623

624 **Table 3. Comparison of Simulated Air-Water Exchange Fluxes to PE-Derived and Grab**

625 **Sample-Derived Exchange Fluxes.**

	Scenario 1: Randomly Fluctuating Air and Water Concentrations	**Scenario 2: Steadily Increasing Air and Decreasing Water Concentrations**
Relative Percent Difference (RPD) between F_{aw} and $F_{aw,PE}$		
Mean F_{aw} Over 100 Days	18.5+/-6.8%	357+/-267%
Mean F_{aw} Over Last 22 days	15.3+/-8.8%	8.4+/-5.2%
F_{aw} on Day 100	351+/-219%	12.3+/-1.2%
Relative Percent Difference (RPD) between F_{aw} and mean F_{aw} from weekly grab sample		
Mean F_{aw} Over 100 Days	26.9+/-15.0%	21+/-15%
Mean F_{aw} Over Last 22 days	60.4+/-34.6%	329+/-232

626

627

628

629

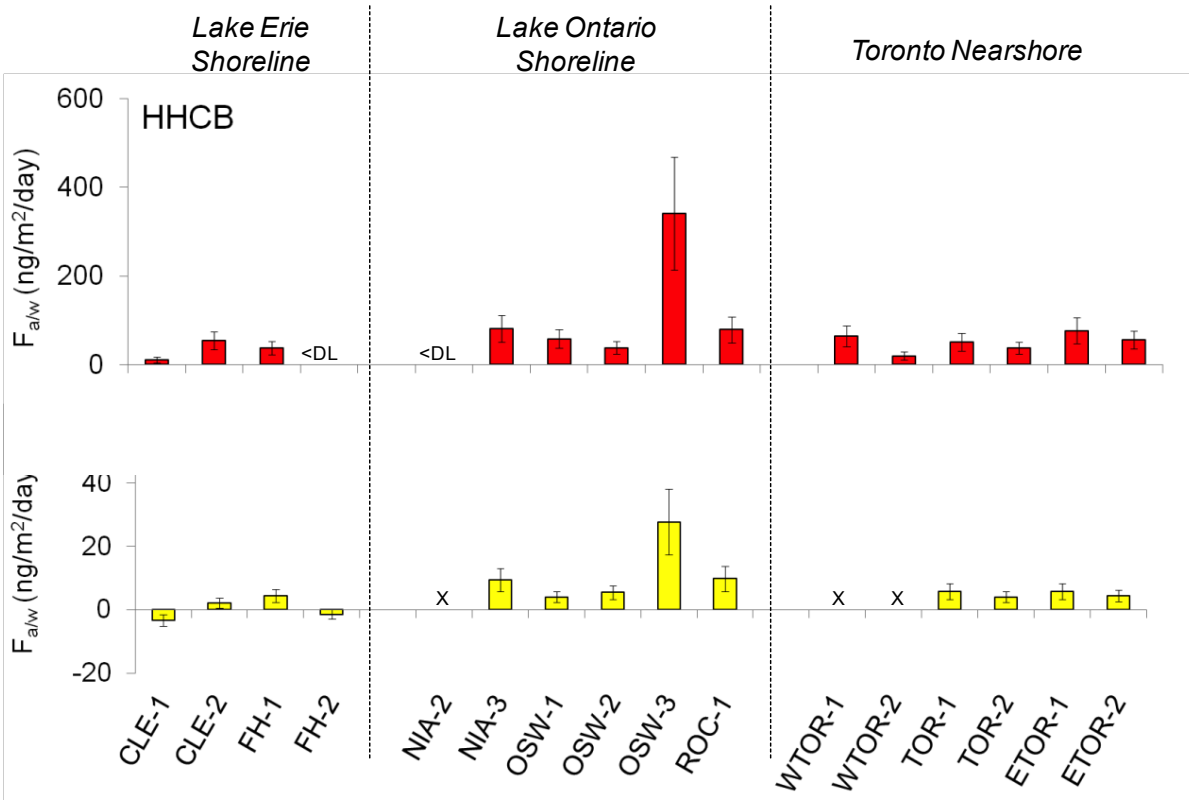

630

631 **Figure 4. Summer air-water exchange fluxes of AHTN and HHCB.** Air-water exchange
632 fluxes are shown for shoreline Lake Erie and Lake Ontario sites, as well as nearshore Toronto
633 buoy sites. Positive bars represent volatilization while negative bars represent absorption. Cases
634 where both air and water concentrations were <DL were marked "<DL". Cases where fugacity
635 ratios were not significantly different from equilibrium were marked "X". Offshore Lake Erie
636 and nearshore northern Lake Ontario sites as well as some shoreline sites (SHF, ERI, DUN,
637 BUF, and CV) were omitted because no significant exchange fluxes were calculated there. Error
638 bars represent standard deviation calculated via error propagation.

639

640

641

642

643

644 **GRAPHICAL ABSTRACT**

645 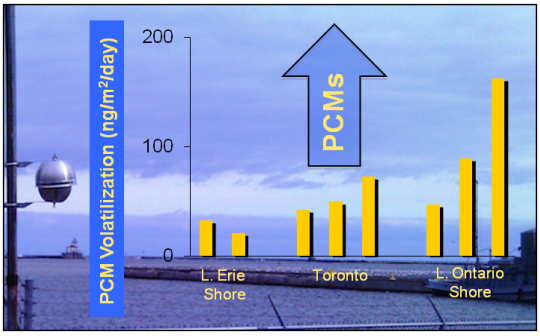

646 For Table of Contents only

647